The Influence of Meso-Substitution on the Photophysical Behavior of Some Thiacarbocyanine Dyes in Dilute Solution

Nadia Vranken, Sven Jordens, Gino De Belder, Marc Lor, Els Rousseau, Gerd Schweitzer, Suzanne Toppet, Mark Van der Auweraer,* and Frans C. De Schryver

Laboratory for Molecular Dynamics and Spectroscopy, Katholieke Universiteit Leuven, Department of Chemistry, Celestijnenlaan 200F, 3001 Heverlee, Belgium

Received: June 20, 2001; In Final Form: August 27, 2001

Fluorescence upconversion experiments were performed on monomer solutions of a number of structurally similar thiacarbocyanine dyes. The results from these time-resolved experiments combined with the data obtained from steady-state absorption and emission and ^{1}H NMR spectra allowed us to assign the components with different decay times to distinct isomers of the thiacarbocyanine dye molecules. Furthermore, it was possible to relate the substitution pattern of the dye molecules to their photophysical properties. For all meso-substituted dyes, a short-lived component of either 3.5 or 5.7 ps could be assigned to a mono-cis conformation of the thiacarbocyanines. This component emits at longer wavelengths. A second component ranging from 15 to 71 ps and emitting at shorter wavelengths was attributed to the all-trans conformation of the meso-substituted trimethine dyes. Time-resolved emission spectra revealed in a very clear and direct way the evolution of the contribution of the two conformations to the spectra. The size and/or solvation of the *N*,*N*′-substituents have a parallel influence on the decay time of the fast and the slow decaying component. Besides the *N*,*N*′-substituents also the meso-substituent has an influence on the decay time and amplitude of the longer-lived component.

Introduction

Cyanine dyes are widely used spectral sensitizers because of their properties such as a high extinction coefficient, strong adsorption onto silver halides, suitable energy levels and the possibility to tune the photophysical properties by minor changes in the dye structure.[1−3] The photophysical properties of dilute solutions, where the dye is, at low concentration, generally present as a monomer, have since long been studied using various techniques. Cis−trans isomerization has been found to play an important role in the excited state of meso-substituted carbocyanines.[4,5]

Fluorescence decay times ranging from several tens of picoseconds to up to three nanoseconds were reported for cyanine dyes.[5−9] While reliable data are available on the meso-unsubstituted carbo- and dicarbocyanines,[5,10] much less unambiguous information is available on the simple cyanines[11] or meso-substituted carbocyanines[12] due to the complexity of the decays and the short decay times.

The work presented here reports on the study of the photophysical properties of a number of thiacarbocyanine dyes dissolved in methanol. To elucidate the role of the substituents, which can strongly influence the photophysical properties,[13] several cyanine dyes with a general structure as depicted in Figure 1 were studied. In this study, the 5,5′-substituents, the 3,3′-substituents, and the 9-substituent on the trimethine bridge were changed (Table 1). Fluorescence decay curves of the methanol solutions of the dyes recorded with a 250 fs response function suggested the coexistence of two different conformations of the meso-substituted dye molecules in solution. Time-resolved fluorescence spectra for **TDC** nicely reveal the evolution of the contribution of the two components to the emission spectrum. To our knowledge, this is the first time such time-resolved spectra are determined for a cyanine dye.

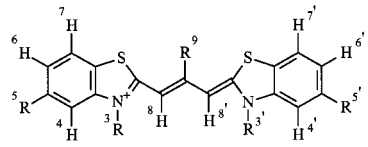

Figure 1. General structure of the studied thiacarbocyanine dyes. The different dyes with this general structure that were studied are summarized in Table 1.

Instrumentation and Sample Preparation

TDC and **THIATS** were gifts from Agfa. The other dyes were synthesized in a straightforward two-step synthesis. The modus and purification has been described elsewhere.[14] The dyes were dissolved in methanol (spectroscopic grade, Aldrich) either in a 10^{-6} M or 10^{-4} M concentration. The photophysical properties of the dilute solutions were measured in 1 cm quartz cuvettes, those of the more concentrated solutions were determined in 1 mm quartz cuvettes. Steady-state absorption spectra were recorded using a double beam UV/VIS spectrophotometer (lambda40-series, Perkin-Elmer Instruments). Steady-state fluorescence spectra were recorded using a standard fluorimeter (Fluorolog 1691, Spex) with correction for the wavelength dependence in the excitation and emission path. Fluorescence quantum yields were determined using as reference a solution of Rhodamine B in ethanol, which has a fluorescence quantum yield of 0.65.[15] The excitation wavelength was either 540, 525, or 495 nm. No influence of the excitation wavelength on the fluorescence spectra or quantum yield was detected.

* Author to whom correspondence should be addressed. Fax: +32(0)16 32 79 90. E-mail: mark.vanderauweraer@chem.kuleuven.ac.be.

10.1021/jp0123536 CCC: $20.00
Published on Web 10/23/2001

TABLE 1: Abbreviations (first column), Substitution Pattern (second, third, and fourth column) and Full Name (last column) of the Studied Thiacarbocyanine Dyes[a]

dye	3,3′-R	5,5′-R	9-R	full name
TD0	Et	H	H	3,3′-diethyl-thiacarbocyanine
TD1	Et	H	Me	3,3′-diethyl-9-methyl-thiacarbocyanine
TD2	Et	H	Et	3,3′-diethyl-9-ethyl-thiacarbocyanine
TDC	Et	Cl	Et	5,5′-dichloro-3,3′-diethyl-9-ethyl-thiacarbocyanine
THIATS	sulfoPro	Cl	Et	5,5′-dichloro-3,3′-disulfopropyl-9-ethyl-thiacarbocyanine
THIA2	sulfoPro	H	Et	3,3′-disulfopropyl-9-ethyl-thiacarbocyanine
THIA1	sulfoPro	H	Me	3,3′-disulfopropyl-9-methyl-thiacarbocyanine
THIA0	sulfoPro	H	H	3,3′-disulfopropyl-thiacarbocyanine

[a] The general structure of the dyes is depicted in Figure 1. For the cationic dyes the counter ion is chloride except for **TDC**, where the counter ion is the tosylate anion, for the overall anionic dyes the triethylammonium ion is the counter ion (Et: ethyl; sulfoPro: sulfopropyl; H: hydrogen; Cl: chloro; Me: methyl).

^{1}H NMR experiments were carried out using a 400 MHz NMR-apparatus (AMX 400, Bruker) in a temperature range between +55 °C and −60 °C. For these experiments the dyes were dissolved in deuterated DMSO, ethanol, or chloroform.

Fluorescence decay curves of the 10^{-6} M dye solutions were recorded using the time-correlated single-photon counting technique (TCSPC) which has been described in detail elsewhere.[16] The excitation was performed at 543 nm. The fluorescence decay curves were recorded at 575, 590, and 605 nm. All decay curves were recorded versus the instrumental response function (IRF) as well as versus the fluorescence decay of 2-[2-[3-(dimethylamino)fenyl]-ethenyl]-*N*-methylpyridinium iodide (DASPI) in methanol (lifetime of 28 ps[17]). The full width at half-maximum (fwhm) of the IRF was typically in the order of 40 ps during these experiments, which results in a time resolution of ca. 15 ps after deconvolution. The time increment per channel was 3 ps for all experiments described here. All experiments were performed under magic angle conditions. All individual decay traces were analyzed as a sum of exponentials using a nonlinear least-squares algorithm.[18,19] The quality of the fits was judged by the values of the reduced χ^2 (<1.3) as well as by the residuals and their autocorrelation function,[20] the heteroscedasticity plot,[21] the RUNS test,[21] and the Durbin Watson test.[22]

To obtain a higher time resolution, fluorescence decay curves of the 10^{-4} M solutions were recorded using the fluorescence upconversion technique. The higher concentration was necessary to arrive at a sufficient absorption at the excitation wavelength in the 1 mm cells used for the upconversion experiments. The setup for these experiments has been described in detail elsewhere.[23,24] The excitation wavelength was set to 495 nm, while the fluorescence decay was collected at four different wavelengths of 560 nm, 570, 590, and 610 nm. The system prompt response was typically in the order of 285 fs for these experiments. Fluorescence decay curves were recorded in three different time windows: 200 ps (with a time increment of 195 fs), 20 ps (with a time increment of 20 fs), and 5 ps (with a time increment of 6.7 fs), to be able to resolve possible fast decaying components. The Levenberg−Marquardt minimization[25] algorithm of a commercial software package (Origin, Microcal) was used to fit the data by a sum of exponentials convoluted with the system prompt response. The fits were judged by inspection of the residuals plots and minimization of the χ'^2.

Results and Discussion

Steady-State Absorption and Fluorescence Spectroscopy Experiments. The steady-state absorption and emission spectra for the 10^{-6} M solutions of the 3,3′-ethyl substituted dyes are shown in Figure 2, the absorption and fluorescence spectra of the corresponding 3,3′-sulfopropyl substituted dyes are identical (data not shown). The spectral data for all dye solutions with this concentration are given in Table 2. The absorption and fluorescence spectra (excited at the same wavelength) of the more concentrated 10^{-4} M solutions were identical to those of the dilute solutions (see Figure 3). As a double check, the fluorescence quantum yields of the concentrated solutions were determined and, within the experimental error, found to be identical to those of the more dilute solutions. No spectral evidence for dimer formation or the formation of higher aggregates was found upon increasing the dye concentration from 10^{-6} M to 10^{-4} M in methanol.

The absorption spectra of all dye solutions show a maximum between 542 and 559 nm and a shoulder at shorter wavelengths (520 nm) which is attributed to a vibrational band (0−1

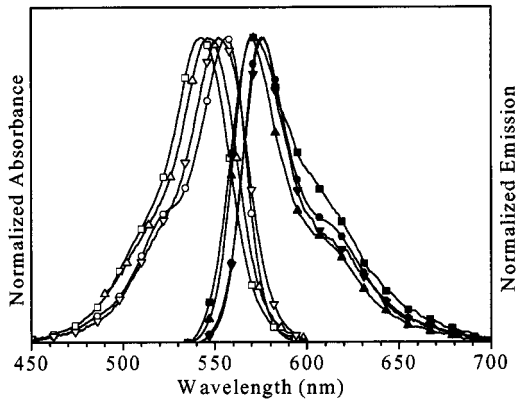

Figure 2. Absorption (open symbols) and emission (corresponding filled symbols) spectra for the 10^{-6} M solutions of **TD0** (●, ○), **TD1** (■, □), **TD2** (▲, △), and **TDC** (▼, ▽) in methanol. The excitation wavelength was 525 nm.

TABLE 2: Spectral Data of the 10^{-6} M Solutions of the Different Dyes Dissolved in Methanol[a]

dye	λ_{abs} (nm)	λ_{em} (nm)	ν (cm^{-1})	FW2/3M$_{abs}$ (cm^{-1})	FW2/3M$_{em}$ (cm^{-1})	ϕ_f	ϵ_{max} (10^5 l/mol cm)
TD0	557	574	530	820	660	0.036	1.7
TD1	542	569	880	1020	910	0.001	1.0
TD2	547	571	770	970	700	0.002	1.2
TDC	552	579	840	950	620	0.002	0.9
THIATS	552	579	840	950	680	0.002	0.9
THIA2	547	573	830	970	660	0.002	1.0
THIA1	543	572	930	920	970	0.002	1.0
THIA0	559	577	560	810	660	0.052	1.6

[a] λ_{abs}, λ_{em}: absorption, emission maximum, respectively; ν: Stokes Shift; FW2/3M$_{abs}$, FW2/3M$_{em}$: bandwidth at 2/3 of the maximum for the absorption and emission spectrum, respectively; ϕ_f: fluorescence quantum yield; ϵ_{max}: molar extinction coefficient at the absorption maximum.

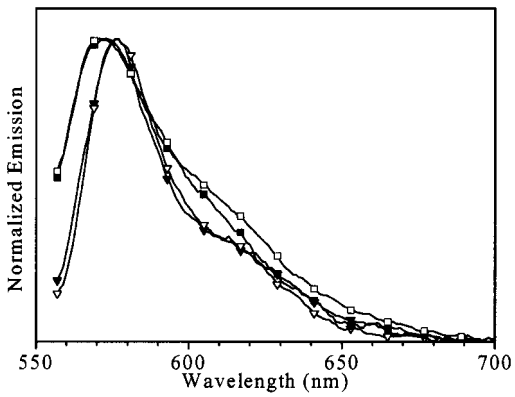

Figure 3. Emission spectra for the 10^{-4} M (open symbols) and 10^{-6} M (corresponding filled symbols) solutions of **TDC** (▼, ▽) and **TD1** (■, □) in methanol. The excitation wavelength was 540 nm.

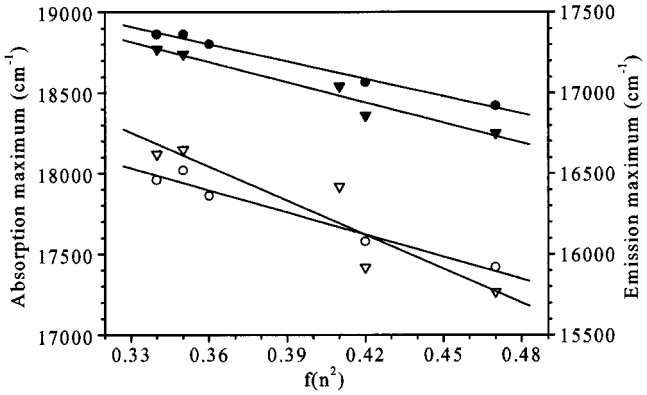

Figure 4. Plot of the absorption maxima (open symbols) and emission maxima (corresponding filled symbols) of **TDC** (▼, ▽) and **TD0** (●, ○) as a function of the solvent parameter $f(n^2)$. The lines are the linear least-squares fits for the different data sets. For the fit of the emission maxima R^2 is 0.96 for **TDC** and 0.99 for **TD0**, for the fit of the absorption maxima R^2 is 0.85 for **TDC** and 0.96 for **TD0**.

vibrational transition). This shoulder is most pronounced for the meso-unsubstituted dyes. The emission spectra are quasi mirror-images of the absorption spectra. The emission maxima are mainly dependent on the polarity/polarizability of the solvent (see below). The steady-state results indicate that **TD0** and **THIA0** have the narrowest and most red-shifted absorption band. Bandwidths are measured at two-thirds of the maximum (FW2/3M) since at half-maximum there might be interference of the vibrational band. **TD1** has the widest and most blue-shifted absorption and emission band. This behavior was also observed for its 3,3′-sulfopropyl analogue **THIA1**, when compared to the other 3,3′-sulfopropyl analogues. The 9-ethyl substituted dyes **TD2**, **TDC**, **THIA2,** and **THIATS** have a wider absorption band than **TD0** and **THIA0**, but they have similar emission bandwidths and a similar emission maximum. However, the fluorescence quantum yield of **TD0** and **THIA0** is 1 order of magnitude larger than for the dyes with a meso-substituent. These observations suggest that the 9-ethyl-substituted dyes are present as a mixture of two isomers.[4] One isomer absorbs at shorter wavelengths, is characterized by a very low fluorescence quantum yield, and is most dominantly present. The other isomer is only present in low quantities and has spectral and fluorescence quantum yield characteristics similar to those of **TD0** or **THIA0**. This assumption is supported by a study of the influence of the solvent on the steady-state spectra of **THIATS**,[12] **TDC** (Figure 4), and **TD0** (Figure 4). Contrary to what is observed for other carbocyanine[5,8] and cyanine dyes,[26] for **TDC** and **THIATS** no correlation could be found between the absorption maxima and the Bayliss parameter[27−29] $f(n^2) = 2(n - 1)/(2n^2 + 1)$, where n is the refractive index of the solvent. For the emission spectra, on the other hand, a linear relation was found between the emission maximum and $f(n^2)$. For **TD0** a linear correlation with the solvent parameter $f(n^2)$ was observed for the emission maxima as well as for the absorption maxima. This indicates that the steady-state absorption as well as the emission spectrum of **TD0** are dominated by a single species. Also for **THIATS** and **TDC**, the steady-state emission spectra are dominated by a single emitting species, causing the small changes of the emission bandwidth as a function of the solvent for the 9-ethyl substituted dyes. The absorption spectra of **THIATS** and **TDC**, on the other hand, reflect the presence of two isomers with a relative abundance dependent on solvent polarity and polarizability.[5,12]

TABLE 3: ^{1}H NMR Chemical Shifts of the Relevant Protons for THIA0, Determined as a Function of Decreasing Temperature in Deuterated Methanol[a]

T (°C)	H_9 (ppm)	$H_{8,8'}$ (ppm)	$H_{4,4'}$ (ppm)	$H_{6,6'}$ (ppm)	$H_{5,5'}$ (ppm)	$H_{7,7'}$ (ppm)
20	7.91	6.62	7.73	7.35	7.52	7.78
10	7.90	6.62	7.72	7.33	7.51	7.78
0	7.87	6.60	7.69	7.29	7.48	7.76
−10	7.81	6.58	7.65	7.21	7.44	7.73
−20	7.73	6.53	7.59	7.11	7.38	7.68
−30	7.64	6.48	7.52	6.98	7.31	7.62
−40	7.54	6.42	7.46	6.85	7.24	7.52
−50	7.47	6.35	7.38	6.77	7.17	7.47
−60	7.28	6.24	7.14	6.24	7.14	7.28

[a] The vinyl-protons (8,8′-position) and the meso-proton (9-position) are situated on the trimethine bridge, $H_{7,7'}$, $H_{6,6'}$, $H_{5,5'}$, and $H_{4,4'}$ are situated on the benzthiazole rings as depicted in Figure 1.

^{1}H NMR Experiments. ^{1}H NMR data, recorded at room temperature, of **TD0** and **THIA0** dissolved in deuterated DMSO (or deuterated methanol) showed a doublet-signal for the vinyl(8,8′)-protons (from the coupling with the meso(9)-proton, which itself is revealed as a triplet in both cases). The calculated coupling constant was 12.8 Hz (12.4 Hz in deuterated methanol) for **TD0** and 12.4 Hz (also 12.4 Hz in deuterated methanol) for **THIA0**. These values are typical for trans-coupled protons, taking into account the substituents on the double bond[30] and were confirmed by Ponterini et al. for a similar oxacarbocyanine dye.[31] These results indicate that the predominant isomer of the meso-unsubstituted thiacarbocyanine dyes **TD0** and **THIA0** (cf., the steady-state experiments) is a quasi-planar all-trans conformation. Extra proof for this assumption could be obtained from temperature-dependent ^{1}H NMR spectra of **THIA0** in deuterated methanol (Table 3) indicating no splitting for the signals of the relevant protons at lower temperatures. Contrary to the observations made for **THIA0**, the ^{1}H NMR spectra of solutions of **THIATS**[12] and **TDC** (Table 4) in deuterated methanol and chloroform revealed, at low temperature, two distinct signals for the vinyl-protons (8,8′-position, on the trimethine bridge) and some of the phenyl-protons. This can be due to the prevalence of a mono-cis isomer, where both vinyl-protons are no longer equivalent for the meso-substituted dyes. Since the integration of both signals for the vinyl-protons revealed an excess of ±25% in favor of the signal at lower field assigned to a proton on a double bond in an E-configuration, it seems reasonable to assume a residual population of ca. 10% for an all-trans isomer where both vinyl-protons are situated on a double bond in an E-configuration. The signal for the $H_{8,8'}$-protons of **THIA0** at lower temperatures corresponds very well with the signal attributed to the proton on a double bond in

TABLE 4: ^{1}H NMR Chemical Shifts of the Relevant Protons for TDC, Determined as a Function of Decreasing Temperature, in Deuterated Methanol and Deuterated Chloroform[a]

CD_3OD					$CDCl_3$				
T (°C)	$H_{8,8'}$ (ppm)	$H_{7,7'}$ (ppm)	$H_{6,6'}$ (ppm)	$H_{4,4'}$ (ppm)	T (°C)	$H_{8,8'}$ (ppm)	$H_{7,7'}$ (ppm)	$H_{6,6'}$ (ppm)	$H_{4,4'}$ (ppm)
55	6.46	7.86	7.41	7.76	55	6.78	7.79	7.22	7.26
35	6.47	7.86	7.41	7.78	35	6.78	7.80	7.22	7.26
25	6.47	7.86	7.40	7.78	20	6.79	7.79	7.22	7.25
10	6.49	7.88	7.41	7.81	0	6.29/7.28	7.65/8.0	7.24	7.24/7.16
−10	6.45	7.86	7.39	7.80	−20	6.25/7.27	7.61/8.0	7.23	7.24/7.18
−30	6.33/6.77	7.89	7.37	7.83	−30	6.24/7.28	7.62/8.0	7.22	7.24/7.16
−50	6.29/6.79	7.89/7.61	7.34/7.21	7.81/7.52	−50	6.22/7.25	7.64/8.0	7.22	7.25/7.15

[a] The vinyl-protons (8,8′-position) are situated on the trimethine bridge, $H_{7,7'}$, $H_{6,6'}$, and $H_{4,4'}$ are situated on the benzthiazole rings as depicted in Figure 1. At lower temperatures (at −30 °C for CD_3OD, at 0 °C for $CDCl_3$) there is a splitting for the signals of the protons, revealing two different conformations of the dye molecule.

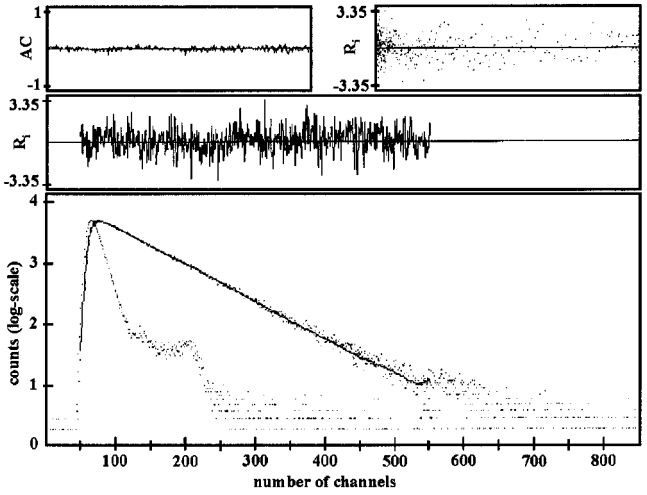

Figure 5. Decay curve (recorded at 575 nm) and reference convoluted fit of a 10^{-6} M solution of **THIA0** in methanol (bottom) with corresponding residuals plot (middle), and autocorrelation function (top left) and heteroscedasticity plot (top right).

E-configuration in **TDC** at low temperature (compare Tables 3 and 4), which is an extra proof for the validity of the assignment of this signal. Henrichs and Ross observed a similar splitting for the signal of the $H_{8,8'}$-protons into a signal at lower and a signal at higher field.[32] They also assigned the new signal at lower field to the proton on a double bond in E-configuration and the signal at higher field to the other proton on the trimethine bridge. It is not likely that this splitting of the signals of the 8- and 8′-protons is due to aggregation. Independently of the formation of H- or J-aggregates[33] both protons, although possibly subject to an upfield shift, should remain equivalent.

Fluorescence Decay Measurements. The steady-state spectra discussed above lead to the assumption of the presence of two different species in dilute solutions of the studied meso-substituted thiacarbocyanine dyes. Furthermore the ^{1}H NMR data indicate that in contrast to the meso-unsubstituted dyes, two different isomers prevail for the meso-substituted dyes. Those data suggest that investigating the photophysical properties of those dyes should reveal two different kinetic species. Thus time-resolved experiments impose themselves, moreover, because only limited consistent data are available in the literature.[6−9,12] Furthermore the time-resolved experiments could give additional information on the influence of the substitution pattern on the photophysical properties of the thiacarbocyanine dyes.

Single-Photon Counting Experiments. Fluorescence decay curves of the 10^{-6} M solutions of all dye molecules investigated in methanol were recorded with the TCSPC setup. The excitation

TABLE 5: Data Retrieved from the Reference Convoluted Fits of the Fluorescence Decay Curves ($I(t) = \alpha_1 \exp(-t/\tau_1) + \alpha_2 \exp(-t/\tau_2) + \alpha_3 \exp(-t/\tau_3)$) Measured with the TCSPC Setup for the Meso-Substituted Thiacarbocyanine Dyes[a]

dye	λ_{em} (nm)	α_1	α_2	α_3	τ_1 (ps)	τ_2 (ps)	τ_3 (ps)	χ^2
TD1	575	0.01	1.50		199	14		1.10
	590	0.01	1.85		218	11		1.00
	605	0.01	1.74		252	12		1.02
TD2	575	0.03	1.92		162	27		1.07
	590	0.02	1.06		133	25		1.00
	605	0.02	1.04		153	23		1.15
THIATS	575	0.09	0.28	3.01	151	64	4	1.01
	590	0.04	0.24	1.10	184	89	12	0.95
	605	0.07	0.19	3.57	157	64	5	1.01
THIA2	575	0.05	0.36	1.64	161	65	8	1.06
	590	0.06	0.27	1.56	151	61	8	1.05
	605	0.03	0.20	1.28	172	69	12	1.06
THIA1	575	0.03	1.01		220	25		1.13
	590	0.03	1.15		214	20		1.19
	605	0.02	0.92		217	19		1.21

[a] λ_{em}: detection wavelength; τ_i: decay times (ps); α_i: corresponding amplitudes; and χ^2 indicates the goodness of the fit.

was done in the main absorption band, at 543 nm, the decay curves were recorded at an emission wavelength near the maximum (575 nm), at an emission wavelength past the maximum (590 nm) and in the red tail of the emission band (605 nm).

The fluorescence decays of **TD0** and **THIA0** could be analyzed as a monoexponential decay with decay times of 130 and 210 ps, respectively (Figure 5 − χ^2: 1.064, time increment per channel: 3 ps, Durbin-Watson parameter: 1.88, Runs-test parameter: 0.040). Combining these decay times with the respective fluorescence quantum yields ($k_f = \phi_f/\tau_f$) gives a fluorescence rate constant for **TD0** of 2.8×10^8 s^{-1} and for **THIA0** of 2.5×10^8 s^{-1}. These values are in very good agreement with fluorescence rate constants obtained for other carbocyanine dyes[5,8] or values obtained by PPP-calculations on the same chromophore.[34] Due to the absence of steric hindrance of a meso-substituent these dye molecules will, in agreement with the ^{1}H NMR results, preferably adopt a quasi planar all-trans conformation.

In contrast to **TD0** or **THIA0**, the fluorescence decay curves of all meso-substituted dyes had to be analyzed as a bi- or triexponential decay. Using reference convolution (Table 5) or fitting the decay curves versus the IRF (data not shown) resulted in similar decay times. To obtain acceptable fits for the decay curves it was always necessary to add a short-lived component with a decay time near, or even smaller than, the experimental

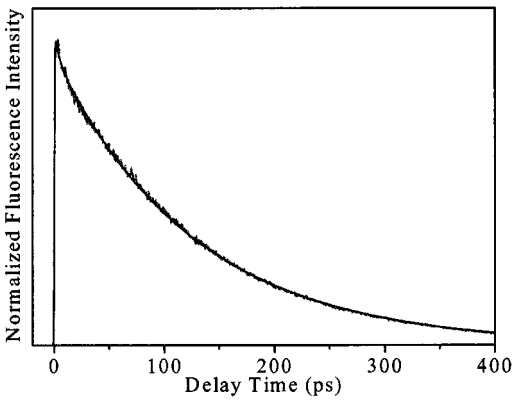

Figure 6. Illustration of the decay trace and the fit for the dye **TD0** recorded with the fluorescence upconversion technique. The detection wavelength was set to 610 nm.

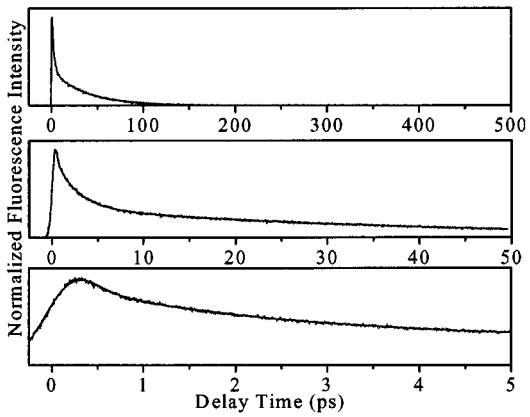

Figure 7. Decay traces and the fits for the dye **TDC** recorded with the fluorescence upconversion technique for the three different time windows. The detection wavelength was set to 560 nm.

resolution of 15 ps. As the latter component could not always be resolved properly it was not attempted to analyze these decays globally, linking the decay times over different emission wavelengths. Instead, the TCSPC data were extended with fluorescence decays obtained by fluorescence upconversion experiments where a much better time resolution of 250 fs (typically) could be reached.

Fluorescence Upconversion Experiments. Although for experimental reasons the samples for fluorescence upconversion had to be excited at 495 nm the steady-state data suggested that this had only a marginal effect on the fluorescence spectra or quantum yields in methanol. The emission was detected at slightly shorter wavelengths than the emission maximum (560 nm), at the emission maximum (570 nm), at slightly longer wavelengths (590 nm), and in the red tail of the emission band (at 610 nm). This allowed us to determine the wavelength dependence of the contribution of the different components to the steady-state emission spectrum.

The decay of **TD0** was recorded in a time window of 420 ps (time increment: 427 fs), to allow a comparison with the TCSPC experiments. The detection wavelength was 610 nm. A bi-exponential decay was found for this dye (Figure 6), with a component of 127 ps (amplitude of 0.95) and a short-lived component of 5.8 ps (amplitude of 0.05). The first component is identical to that found for the TCSPC experiments and is attributed to the fluorescence decay of the all-trans conformation of the dye molecules. The short-lived component was not resolved accurately during these experiments due to the limited time resolution and the small relative amplitude of this component. It could be attributed to fluorescence of a mono-cis isomer, since the occurrence of this conformation has already been proven for meso-unsubstituted dyes.[31,35] The small relative amplitude of this component explains why it is not observed in the ^{1}H NMR data or the steady-state absorption and fluorescence spectra nor in the fluorescence quantum yield. This fast-decaying component might, however, also be attributed to a number of other possible processes, such as internal vibrational reorganization (IVR), vibrational relaxation, solvent relaxation, or singlet annihilation. The formation of photoproducts (except the cis-isomer) is highly unlikely as the excitation power was not high enough to result in an observable bleaching of the samples. To be able to evaluate the processes of IVR, vibrational relaxation or solvent relaxation decay traces at a large number of different detection wavelengths are necessary, to determine the wavelength dependence of the amplitude of this second component.

The decays of the meso-substituted dyes **TD1**, **TD2**, **TDC,** and **THIATS** had to be fitted as a sum of three exponentials (Figure 7). A first component had a sub-picosecond decay time, a second component had a decay time of several picoseconds, and the third component had a decay time of a few tens of picoseconds. All data retrieved from the decay analysis are summarized in Table 6. For each dye the decay curves were globally analyzed over the different detection wavelengths.

While the amplitude (α_1) of the sub-picosecond decay time (τ_1) was found to be large and positive at lower emission wavelengths, it became progressively smaller and even negative at longer wavelengths. This evolution for α_1 points in the direction of an IVR process as this decay time τ_1 is clearly related to a generating process for the species with the decay time τ_2 or τ_3 emitting at longer wavelengths. It was only possible to link this decay time τ_1 over the different emission wavelengths for the dyes **TD1** and **THIATS**. The similarity of the first decay time τ_1 for these structurally different thiacarbocyanine dyes (1.0 ± 0.2 ps) indicates that this short-lived component is due to the same process for all investigated meso-substituted dyes.

The decay times of the second and the third component (τ_2 and τ_3) could be linked over the different emission wavelengths for all studied meso-substituted dyes. The decay time for the second component was, within the experimental error, identical for the 3,3′-ethyl substituted dyes **TD1**, **TD2**, and **TDC**, namely, 3.5 ± 0.3 ps. For the 3,3′-sulfopropyl substituted dye **THIATS** the decay time for the second component was determined at 5.7 ps. For all meso-substituted dyes the relative amplitude for this second and third component was recalculated ($\alpha_2/(\alpha_2 + \alpha_3)$ and $\alpha_3/(\alpha_2 + \alpha_3)$), neglecting the amplitude of the first decay time, due to a generative process. The amplitude ($\alpha_2/(\alpha_2 + \alpha_3)$) becomes larger ($\geq 0.8$) at longer detection wavelengths (Table 6), where it is clearly the most important component.

For the meso-unsubstituted dyes **TD0** and **THIA0** the most important decay results from the fluorescence of a long-lived component attributed to the all-trans conformation of the dye molecules. The ratio between the decay times τ_2 of the most abundant component of **TDC** and **THIATS** equals 0.6 and is the same as the ratio between the decay times of the major component of **TD0** and **THIA0**. Relating this with the difference in substitution pattern of the dyes suggests that a more bulky and/or more solvated (because of the negative charge on the sulfopropyl group) 3,3′-substitution increases the decay time. Similar results were found for meso-unsubstituted oxacarbocyanine and indolocarbocyanine dyes.[5,9,36]

The decay time of the more slowly decaying third component (τ_3) decreases from 71 ps for **THIATS,** to 39 ps for **TDC,** to

TABLE 6: Data Retrieved from Global Analysis of the Fluorescence Decay Curves Measured with the Setup for Fluorescence Upconversion for the Meso-Substituted Thiacarbocyanine Dyes[a]

dye	λ_{em} (nm)	α_1	α_2	α_3	τ_1 (ps)	τ_2 (ps)	τ_3 (ps)	$^A\alpha_2/(\alpha_2+\alpha_3)$	$^A\alpha_3/(\alpha_2+\alpha_3)$	$^B\alpha_2\tau_2/(\alpha_2\tau_2+\alpha_3\tau_3)$	$^B\alpha_3\tau_3/(\alpha_2\tau_2+\alpha_3\tau_3)$
TDC	560	1.74	0.30	0.34	0.1	3.8	39	0.48	0.52	0.08	0.92
	570	2.36	0.40	0.42	0.1	3.8	39	0.49	0.51	0.08	0.92
	590	−0.27	0.91	0.37	0.9	3.8	39	0.71	0.29	0.19	0.81
	610	−0.38	1.04	0.30	1.1	3.8	39	0.77	0.23	0.25	0.75
TD2	560	3.43	0.40	0.30	0.1	3.1	30	0.58	0.42	0.12	0.88
	570	0.24	0.57	0.34	0.3	3.1	30	0.62	0.38	0.15	0.85
	590	−0.37	1.00	0.27	1.3	3.1	30	0.79	0.21	0.28	0.72
	610	−0.43	1.10	0.25	1.1	3.1	30	0.82	0.18	0.31	0.69
TD1	560	0.49	0.49	0.26	0.8	3.6	15	0.65	0.35	0.31	0.69
	570	−0.04	0.67	0.30	0.8	3.6	15	0.69	0.31	0.35	0.65
	590	−0.10	0.97	0.29	0.8	3.6	15	0.77	0.23	0.44	0.56
	610	−0.17	1.07	0.28	0.8	3.6	15	0.80	0.20	0.48	0.52
THIATS	560	0.29	0.62	0.15	1.1	5.7	71	0.81	0.19	0.25	0.75
	570	0.20	0.68	0.23	1.1	5.7	71	0.75	0.25	0.19	0.81
	590	−0.20	0.94	0.21	1.1	5.7	71	0.82	0.18	0.26	0.74
	610	−0.34	1.06	0.18	1.1	5.7	71	0.85	0.15	0.32	0.68

[a] λ_{em}: detection wavelength, τ_i: decay times (in ps); α_i: corresponding amplitudes, *A*: relative amplitudes (the first component is not taken into account), *B*: $\alpha_i\tau_i/\Sigma\alpha_i\tau_i$ (the first component is not taken into account).

30 ps for **TD2,** to 15 ps for **TD1**. The relative amplitude of this third component decreases from nearly 0.5 to about 0.2 with increasing detection wavelength, for **THIATS**; however, this evolution is much less pronounced. It seems reasonable to state that the decay times of the second and third component are the same for the dyes **TDC** and **TD2**, hence the 5,5′-substituents have only a minor influence on the fluorescence decay behavior of the studied dyes. This was already observed in the steady-state spectroscopy experiments, in which the absorption and the emission spectra and the fluorescence quantum yields are nearly identical for this series of dyes. In analogy to the observations for the second component an increased decay time is observed with increased bulkiness and/or solvation of the 3,3′-substituents for the third component. Therefore the meso-substituent as well as the 3,3′-substituents have an influence on the decay time τ_3, whereas the decay time τ_2 only seems to be influenced by the 3,3′-substituents.

From the fluorescence quantum yields and the values of the average fluorescence lifetime $\langle\tau_f\rangle$ (estimated according to $\langle\tau_f\rangle = (\alpha_2\tau_2 + \alpha_3\tau_3)/(\alpha_2 + \alpha_3)$) an estimate for the fluorescence rate constant ($k_f = \phi_f/\langle\tau_f\rangle$) of the meso-substituted dyes could be made, assuming that this fluorescence rate constant is the same for the components with decay times τ_2 and τ_3, respectively. For all meso-substituted dyes the estimated value for k_f is ca. 1×10^8 s^{-1}. The difference between the fluorescence rate constant for the meso-substituted dyes and those for the meso-unsubstituted analogues **TD0** or **THIA0** could be due to a decreased planarity on the S_1-surface of the meso-substituted dyes with respect to the more planar meso-unsubstituted dyes. This value of 1×10^8 s^{-1} is merely a lower limit, since in these calculations α_2 and α_3 were both taken to be 0.5. This leads, however, to an underestimation of the fast decaying component, especially at longer wavelengths, where $\alpha_2 > \alpha_3$. Furthermore the emission spectrum of the mono-cis isomer seems to be broader (see Figure 8) which spreads the fluorescence over a larger range of wavenumbers. Although the oscillator strength of the mono-cis isomer is smaller than that of the all-trans isomer, the reduction is probably less than the 2/3 estimated above. Therefore, the amplitudes of the components in the fluorescence decay reflect an overestimation of the all-trans isomer. This brings the time-resolved experiments in better agreement with the ^{1}H NMR experiments.

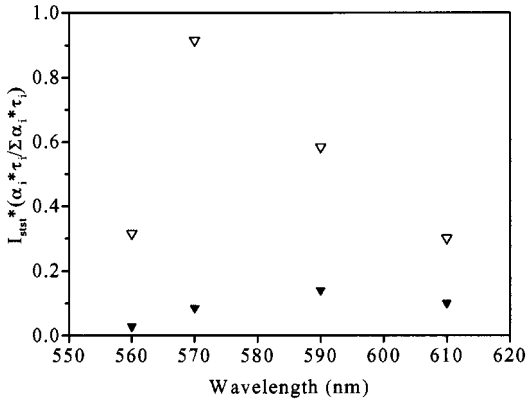

Figure 8. Plot for the dye **TDC** of $\alpha_2\tau_2/(\alpha_2\tau_2 + \alpha_3\tau_3)$ (▼) and $\alpha_3\tau_3/(\alpha_2\tau_2 + \alpha_3\tau_3)$ (▽), both corrected for the normalized steady-state fluorescence intensity. This plot indicates the contributions of the two components determined from the time-resolved experiments to the steady-state emission spectrum.

The relative amplitude of the second component increases with longer wavelengths relative to that of the third component as shown in Table 6, in which the relative amplitudes of both components weighed by the decay times are given. This allowed us to calculate the contribution of both species to the steady-state emission spectrum. Those data reveal that the contribution of the second component to the steady-state emission spectrum is small but becomes more important at longer wavelengths. In Figure 8 the corresponding contributions to the emission spectrum are given for **TDC**, taking into account the wavelength dispersion of the total emission spectrum. Those results indicate that the emission spectrum of the second component is more red shifted and broader than that of the long-living component. Although the nonradiative decay of the excited dye molecules often implicates cis−trans isomerization, there is no indication of an adiabatic conversion of an excited trans to an excited cis isomer.[13,31,35] This means that the fluorescence decay times correspond to the fluorescence lifetimes of the different isomers. Furthermore, the preexponential factors of the decays are only determined by the relative abundance of the cis and trans isomers in the ground state, the ratio of the spectral densities at the emission wavelengths, and the ratio of the fluorescence rate constants. Hence the decay-associated spectra shown in Figure 8 are also species-associated spectra.

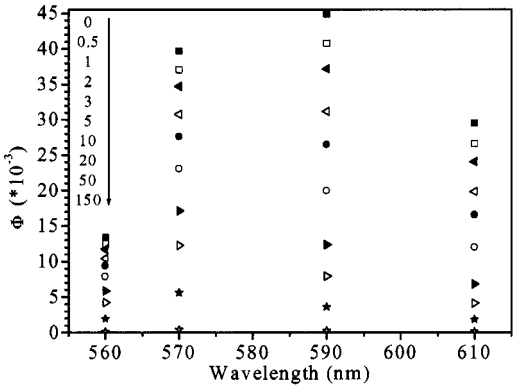

Figure 9. Evolution of the quantum flux functions of **TDC** in the first 150 ps after excitation. The excitation wavelength was 495 nm. Inset: time after excitation (ps) top-to-bottom values correspond to top-to-bottom quantum flux functions.

The fluorescence quantum flux function $\Phi(t,\lambda)$ is defined by expression 1:

$$\Phi(t,\lambda) = \frac{f(t,\lambda)\, F(\lambda)\phi_f}{\int_0^\infty f(t,\lambda)\, dt \int_0^\infty F(\lambda)\, d\lambda} \qquad (1)$$

In this expression is $f(t,\lambda)$ the decay curve corrected for the system prompt response, $F(\lambda)$ is the normalized steady-state fluorescence spectrum, and ϕ_f is the fluorescence quantum yield. A plot of $\Phi(t,\lambda)$ as a function of the emission wavelength, at fixed times, is proportional to the time-dependent spectrum.[25] A number of such plots, at different times after excitation, would visualize even better the evolution of the emission spectrum and the spectral properties of the different components present in the fluorescence decay.

An example of such time-resolved spectra is given in Figure 9, for the dye **TDC**. This plot shows that immediately after excitation the spectrum is dominated by a red-emitting species. But already after less than 5 ps the contribution of a species emitting at shorter wavelengths is dominating the spectrum. This plot confirms the presence of two emitting species, of which the red-emitting species has a fast decay time (less than 5 ps), whereas the blue-emitting species decays on a longer time scale of several tens of picoseconds (less than 100 ps). The large difference in decay times of both species (1 order of magnitude) combined with a similar fluorescence rate constant explains why the steady-state emission spectrum only reflects the emission spectrum of the slowly decaying component. On the other hand the large amplitude of the species decaying with the decay time τ_2 explains why the fluorescence quantum yield of the meso-substituted dyes is much smaller than that of the meso-unsubstituted dyes **TD0** and **THIA0**. The decay time τ_2 is attributed to the fluorescence decay of a mono-cis conformation of the meso-substituted dye molecules. The third component is, in turn, attributed to the fluorescence decay of an all-trans conformation with less steric hindrance and a better planarity, leading to a slower fluorescence decay.[5]

Conclusions

Steady-state spectroscopy experiments and ^{1}H NMR experiments on monomer solutions of a number of structurally very similar thiacarbocyanine dyes indicate the presence of two species that have a different kinetic behavior. Time-resolved fluorescence decays with a 250 fs response function reveal the presence of three components for the studied meso-substituted thiacarbocyanine dyes. The first component has a decay time of around 1 ps. Its amplitude is positive at wavelengths shorter than the emission maximum, and it becomes progressively negative at wavelengths longer than the emission maximum. This suggests that the first decay time is related with a generative process (vibrational or solvent relaxation) for the species with the decay times τ_2 and τ_3. This decay time τ_2 is found to be 3.5 $\pm$ 0.3 ps for the studied meso-substituted *N*,*N*′-ethyl dyes and 5.7 ps for the meso-substituted *N*,*N*′-sulfopropyl dye **THIATS**. From time-resolved spectra it can be concluded that this component emits at longer wavelengths. The decay time of this component can be said to be mainly influenced by the size and/or the solvation of the *N*,*N*′-substitution. No influence of the meso-substitution (ethyl or methyl) was found for the studied *N*,*N*′-ethyl dyes. The decay time τ_3 of the third component changes from 71 to 15 ps. Time-resolved spectra show that this component emits at shorter wavelengths. τ_3 is influenced both by the size and/or solvation of the *N*,*N*′-substitution and by the meso-substituent. With these experiments the presence of two conformations is confirmed for monomer solutions of meso-substituted thiacarbocyanine dyes. Not only was it possible to quantify the decay times of these conformations, it was also possible to visualize the spectral evolution of these two conformations as a function of time.

Acknowledgment. N.V. thanks the "Vlaams instituut voor de bevordering van het wetenschappelijk en technologisch onderzoek" (IWT). The authors gratefully acknowledge the continuing support from DWTC (Belgium) through grant IUAP-IV-11, the F.W.O.-Vlaanderen and the Nationale Loterij and the Research Council of the KULeuven through GOA '96/1. The authors are grateful to Agfa N.V. for the gift of the dyes **THIATS** and **TDC**.

References and Notes

(1) Maskasky, J. E. *Langmuir* **1991**, *7*, 407.
(2) Tani, T.; Suzumoto, T.; Kemnitz, K.; Yoshihara, K. *J. Phys. Chem.* **1992**, *96*, 2778.
(3) Brumbaugh, D. V.; Muenter, A. A.; Horn, L. A.; Adams, K. *YS&T 47th Annu. Conf. ICPS* **1994**, 274.
(4) West, W.; Pearce, S.; Grum, F. *J. Phys. Chem.* **1967**, *71* (5), 1316.
(5) Van der Auweraer, M.; Van den Zegel, M.; Boens, N.; De Schryver, F. C.; Willig, F. *J. Phys. Chem.* **1986**, *90*, 1169.
(6) Dempster, D. N.; Morrow, T.; Rankin, R.; Thomson, G. F. *Faraday Trans. 2* **1972**, *68*, 1479.
(7) Sibbet, W.; Taylor, J. R.; Welford, D. *J. Quantum Electron.* **1981**, *17* (4), 500.
(8) Bendt, K.; Dürr, H.; Feller, K.-H. *Z. Phys. Chem.* **1987**, *268*, 250.
(9) Pevenage, D.; Corens, D.; Dehaen, W.; Van der Auweraer, M.; De Schryver, F. C. *Bull. Soc. Chim. Belg.* **1997**, *106* (*9*−*10*), 562.
(10) Sahyun, M. R. V.; Serpone, N. *J. Phys. Chem. A* **1997**, *101*, 9877.
(11) Tredwell, C. J.; Keary, C. M. *Chem. Phys.* **1979**, *43*, 307.
(12) Noukakis, D.; Toppet, S.; Van der Auweraer, M.; De Schryver, F. C. *J. Phys. Chem.* **1995**, *99*, 11860.
(13) Khimenko, V.; Chibisov, A. K.; Görner, H. *J. Phys. Chem. A* **1997**, *101*, 7304.
(14) Müller, E.; Bayer, O.; Meerwein, H.; Ziegler, K. *Methoden der Organischen Chemie*, 4th ed.; Houben-Weyl, 1972; p 253.
(15) Eaton, D. F. *Handbook of Organic Photochemistry*; CRC Press: Boca Raton FL, Scaiano J. C.; 1989.
(16) Maus, M.; Rousseau, E.; Cotlet, M.; Schweitzer, G.; Hofkens, J.; Van der Auweraer, M.; Krüger, A.; De Schryver, F. C. *Rev. Sci. Instrum.* **2001**, *72* (1), 36.
(17) Hofkens, J. Ph.D. Thesis, Katholieke Universiteit Leuven, 1993.
(18) Marquardt, D. W. *J. Soc. Indust. Appl. Math.* **1963**, *11*, 431.
(19) Gunst, R. F.; Mason, R. L. *Regression Analysis and its Application, A Data-Oriented Approach*; Marcel Dekker: New York, 1980.
(20) Grinvald, A.; Steinberg, I. Z. *Anal. Biochem.* **1974**, *59*, 583.
(21) Caterall, D. *Time-Resolved Spectroscopy in Biochemistry and Biology*; Cundall, R. B., Dale, R. E., Eds.; Plenum Press: New York, 1983.
(22) Durbin, J.; Watson, G. S. *Biometrika* **1950**, *37*, 409; *ibidem* **1951**, *38*, 159; *ibidem* **1971**, *58*, 1.
(23) Schweitzer, G.; Xu, L.; Craig, B.; De Schryver, F. C. *Opt. Commun.* **1997**, *142*, 283.

(24) Karni, Y.; Jordens, S.; De Belder, G.; Hofkens, J.; Schweitzer, G.; De Schryver, F. C.; Herrmann, A.; Müllen, K. *J. Phys. Chem. B* **1999**, *103* (43), 9378.
(25) Karni, Y.; Jordens, S.; De Belder, G.; Schweitzer, G.; Hofkens, J.; Gensch, T.; Maus, M.; De Schryver, F. C.; Hermann, A.; Müllen, K. *Chem. Phys. Lett.* **1999**, *310*, 73.
(26) West, W.; Geddes, A. L. *J. Phys. Chem.* **1964**, *68*, 8 (4), 837.
(27) Bayliss, N. S. *J. Chem. Phys.* **1950**, *18*, 292.
(28) Lippert, E. *Z. Naturforsch.* **1955**, *10A*, 541.
(29) Mataga, N.; Kaifu, Y.; Koizumi, M. *Bull. Chem. Soc. Jpn.* **1955**, *28*, 690.
(30) Williams, D. H.; Fleming, I. *Spectroscopic Methods in Organic Chemistry*, 5th ed.; McGraw-Hill Book Company: London, 1995; p 94.
(31) Ponterini, G.; Momicchioli, F. *Chem. Phys.* **1991**, *151*, 111.
(32) Henrichs, P. M.; Gross, S. *J. Am. Chem. Soc.* **1976**, *98* (23), 7169.
(33) Asanuma, H.; Ogawa, K.; Fukunaga, H.; Tani, T.; Tanaka, J. *Final Program and Proceedings ICPS '98 International Congress on Imaging Science*; Antwerp, Belgium, **1998**, *1*, 178.
(34) Van der Auweraer, M.; Scheblykin, I. *Chem. Phys.*, accepted.
(35) Di Paolo, R. E.; Scaffardi, B.; Duchowicz, R.; Bilmes, G. M. *J. Phys. Chem.* **1995**, *99*, 13796.
(36) Oster, G.; Nishijima, Y. *J. Am. Chem. Soc.* **1956**, *78*, 1581.